ULTRASONIC EXPOSIMETRY

Ultrasonic exposimetry refers to the measurement and characterization of ultrasound fields, primarily as used in medical applications. Because of the similarities between ultrasound sources used in medicine and nondestructive evaluation of materials, some of the concepts discussed here are applicable to this latter area of endeavor as well.

At the outset, the reader should note the subtle distinction between exposimetry and the related term, dosimetry. Exposimetry is concerned with determining the characteristics of an ultrasonic field, but not with the biological consequences of that field. This characterization usually is performed using water as the propagation medium, leading to so-called *free-field* exposure measurements. (An idealized free field would require a homogeneous isotropic medium having no reflective boundaries.) Finding exposure levels in tissue at clinically relevant sites results in either in situ exposure quantities, if measured directly, or estimated in situ exposure values, if calculations are made based on free-field measurements coupled with appropriate tissue models.

In contrast to exposure, the concept of ultrasonic dose (and dosimetry) involves determining the possible production of a biological effect as a consequence of an ultrasonic exposure. None of the three types of exposure quantities identified above, free-field, in situ, or estimated in situ, can be considered arbitrarily a dosimetric quantity. To relate exposure and dose, the site-specific biological consequences of a given exposure and relevant tissue characteristics must be known. The same exposure may create different biological effects, depending on the nature of the tissue exposed.

In this article the main emphasis is on the more fully developed subject of ultrasonic exposure measurements, although where appropriate the progress that has been made in identifying dosimetric quantities is mentioned. The topics covered include a description of the quantities measured or derived, devices and techniques for determining these quantities, methods of calibration, and international and national standards. Emphasis is placed on those devices and techniques that have found the widest use. In particular, topics related to ultrasonic hydrophones are stressed because of their prominence in exposure measurements. The presentation of this material relies heavily on several previous publications to which the interested reader is referred for more in-depth treatments (1–4). These publications also contain a comprehensive list of references, making them valuable to engineers and scientists having various levels of expertise in the field of medical ultrasonics. For more recent works, specific references are given in this article.

MEASUREMENT QUANTITIES

For a complete description of an ultrasonic field, both the temporal and spatial characteristics of the ultrasonic waves must be determined. In this section the most important of the quantities used for this characterization are described, particularly with regard to assessing effectiveness and safety issues in medical applications. This information is based on measurement and calibration standards given in the last section of this article.

Temporal Quantities

A basic quantity for describing the physical nature of an ultrasonic wave is acoustic pressure, defined as the instantaneous change in pressure from the ambient pressure produced by the wave at a particular location. To illustrate how the temporal behavior of an ultrasonic field is quantified, consider the pulsed pressure waveform [i.e., pressure versus time, or $p(t)$] given in Fig. 1(a). This pulse represents the temporal pressure variations at a particular point in the ultrasonic field. It is typical of that encountered in medical imaging, but it can be used to introduce many of the temporal waveform concepts relevant to therapeutic, Doppler, and lithotripsy applications as well. Note that both continuous wave (CW) and pulsed fields are used in medical ultrasound applications. Long pulses (i.e., those many cycles in duration) are found in some therapeutic applications. Short pulses are characteristic of diagnostic and lithotripsy fields.

Pressure

Peak Pressures. The maximum instantaneous compressional and rarefactional pressures are denoted p_c or p_+, and p_r or p_-, respectively. The SI unit is the pascal (Pa), which is equal to one newton per square meter. Note that the pulse shown in Fig. 1(a) is asymmetric with respect to the time axis, causing p_c to be greater than p_r. In a diffracted field this effect is caused by finite amplitude distortion, a phenomenon common to large-amplitude medical ultrasound fields that results in a peaking of the compressional half-cycles and a rounding of the rarefactional half-cycles. At lower pressure amplitudes,

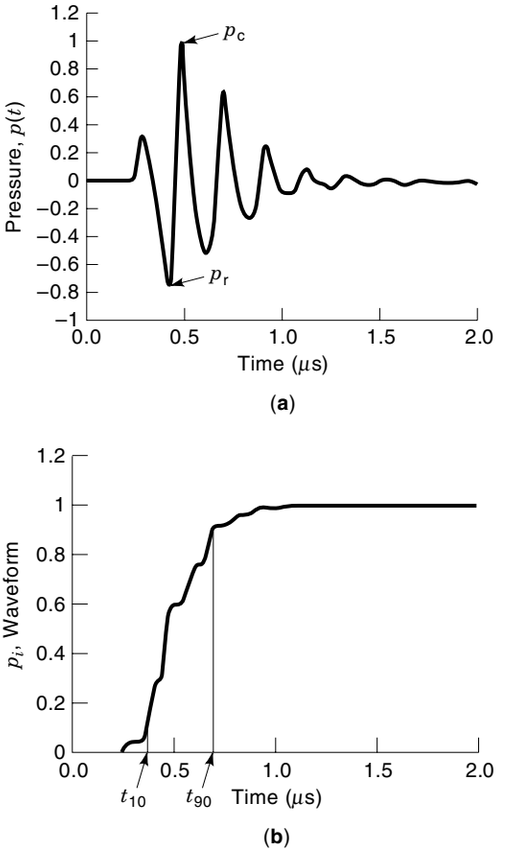

Figure 1. Pressure waveforms (normalized to a maximum value of unity). (a) Typical diagnostic ultrasound pressure pulse; (b) pulse pressure-squared integral (p_i) waveform.

this pulse would look more like a modulated sine wave, with positive and negative pressure excursions being approximately equal.

Another pressure quantity of interest is the fundamental pressure amplitude, p_F. It is equal to the amplitude of the fundamental component of the frequency (Fourier) spectrum of the pulse in Fig. 1(a). For a pulse such as in Fig. 1(a), $p_r < p_f < p_c$; for an undistorted pulse, $p_r = p_f = p_c$.

Pulse Pressure-Squared Integral. The integral of the square of $p(t)$ is called the pulse pressure-squared integral, p_i [Fig. 1(b)]; that is

$$p_i = \int p^2(t)\,dt \tag{1}$$

The limits of integration encompass all nonzero portions of the pulse. Units are pascal squared-seconds (Pa^2s).

Pulse Duration. For diagnostic ultrasound pulses, the pulse duration, PD or t_d, is defined as 1.25 times the interval beginning when the time integral of the square of the instantaneous pressure reaches 10% of its final value and ending when this integral reaches 90% of its final value. This final value is the pulse pressure-squared integral. Referring to Fig. 1(b), PD = $1.25(t_{90} - t_{10})$.

For the pressure pulses encountered in extracorporeal shock-wave lithotripsy, this definition is not as useful because of the long and slowly varying negative tail that is characteristic of these pulses. Therefore, for lithotripsy pulses a compressional pulse duration has been defined as the time beginning at the first time the instantaneous pressure exceeds 50% of the peak-positive pressure and ending at the next time the instantaneous pressure has that value.

For ultrasonic therapy pulses, a third definition is used to account for cases of incomplete modulation; that is, cases in which the pressure amplitude does not return to zero between pulses. Here the pulse duration is the time interval between points on the pressure waveform at which the pressure amplitude first crosses and last reaches a reference level. This reference level is defined as the minimum pressure amplitude plus 10% of the difference between the maximum and minimum pressure amplitudes. The ultrasonic therapy pressure waveform usually is considered to be a modulated sine wave and thus pressure amplitude refers to the peak value of the sinusoidal (carrier) signal during a cycle.

Rise Time. For lithotripsy pulses, the rise time, t_r, is defined as the time taken for the instantaneous pressure to increase from 10 to 90% of the peak-positive pressure.

Pulse Repetition Frequency. The pulse repetition frequency (PRF) is the number of identical pressure pulses generated per second. The reciprocal of the PRF is the pulse repetition period. For diagnostic imaging systems that automatically scan the ultrasonic beam, a quantity related to the PRF is the scan repetition frequency, or SRF. The SRF is the number of scans generated per second.

Center Frequency. The center frequency, f_c, also known as the acoustic working frequency, f_{awf}, is the arithmetic mean of the two most widely separated frequencies at which the Fourier spectrum of the pressure pulse becomes 3 dB lower than its peak value.

Intensity. For a progressive wave, intensity is the acoustic power transmitted in the direction of acoustic wave propagation per unit area normal to this direction. It has units of watts per square meter (or more frequently W/cm^2 or mW/cm^2). Under the common assumption of plane or spherical progressive waves, the instantaneous intensity at a point in the field, $i(t)$, and pressure are related by

$$i(t) = p^2(t)/\rho c \tag{2}$$

where ρ and c are respectively the density and longitudinal wave velocity in the propagation medium. (The product ρc is termed the characteristic acoustic impedance.) This assumption is valid in the far field of an unfocused acoustic source, and near and beyond the focus for a focused source, so it is useful for many situations of practical interest.

Pulse Intensity Integral. Analogous to the pulse pressure-squared integral is the pulse intensity integral, PII or I_{pi}. It is the energy per unit area per pulse and is found by integrating $i(t)$ over all nonzero portions of the pulse. Thus PII = $p_i/\rho c$. The PII has units of joules per square centimeter (J/cm^2).

Temporal-Average Intensity. The temporal-average intensity, I_{TA}, is the time-average of the instantaneous intensity at a point in space. For an unscanned (fixed) ultrasound beam, it is the product of the pulse intensity integral and the pulse repetition frequency. For automatically scanned beams, it is a function of the scan repetition frequency, and the average

includes the contributions from adjacent scan lines that overlap the point of measurement.

Pulse-Average Intensity. The pulse-average intensity, I_{PA}, is the instantaneous intensity averaged over the duration of the pulse. It is equal to the pulse intensity integral divided by the pulse duration.

Displacement. A particle in a medium through which an ultrasonic wave propagates is displaced about its equilibrium position. For linear acoustic plane waves, the acoustic pressure $p(t)$ and particle velocity $v(t)$ at a point are related by $p(t) = \rho c v(t)$. Note: $v(t)$ should be distinguished from the velocity of the wave in the propagation medium, c, as used in Eq. (2). The particle velocity is the time derivative of the particle displacement, $\xi(t)$, so if $\xi(t)$ varies sinusoidally with time, that is, $\xi(t) = \xi_0 \sin(2\pi f t)$, then

$$\xi_0 = p_0/2\pi f \rho c \tag{3}$$

where ξ_0 and p_0 are the particle displacement and pressure amplitudes, respectively, and f is the ultrasonic frequency.

Spatial Quantities

Acoustic pressure and intensity are point quantities, and thus can vary in space as well as time. Both circular and rectangular transducers or transducer arrays are used in medical ultrasound applications. Spatial field distribution measurements of the beams generated by these transducers yield two useful quantities, beam area and beam width. The beam area is defined as the area of the surface in a plane normal to the direction of propagation consisting of the points at which the pulse pressure-squared integral is greater than a specified fraction of the maximum pulse pressure-squared integral. A common value for the fraction is 0.25, or -6 dB, and the area is then denoted A_{-6}. For rectangular beam geometries, two orthogonal beamwidths usually are measured and specified.

Combined Quantities

Additional definitions are useful for quantities that vary in both time and space, such as pressure and intensity. For instance, the temporal-average intensity at the point where it is a maximum is denoted I_{SPTA}, the spatial-peak temporal-average intensity. Similarly, I_{SPPA} is the spatial-peak pulse-average intensity. Spatial-average combined quantities such as I_{SATA} also have been defined. In this case the surface over which the spatial average is taken must be specified.

Ultrasonic Power

The ultrasonic power is the total power radiated by a source transducer into a specified medium, usually water. Although the power varies instantaneously, the temporal-average power, W, is the quantity most often measured and specified.

The temporal-average power and temporal-average intensity are related by the surface integral

$$W = \int_S I_{TA}(r)\, dS \tag{4}$$

where $I_{TA}(r)$ represents the temporal average intensity as a function of spatial coordinate r, and S, the surface of integration, is normal to the direction of propagation.

Estimates of Exposure Quantities In Situ

Derated Quantities. All of the quantities described above typically are measured in water. Water is used for several reasons. It is easily obtainable and its basic chemical and physical properties are well known. With properties such as electrical conductivity, temperature, and gas content specified, it is possible to assure stable and reproducible behavior of the propagation medium at different measurement sites. Also, the acoustic impedance of and wave velocity in water closely approximate those of typical mammalian soft tissues.

This last point is important when trying to predict or extrapolate exposure levels in tissue from measurements made in water. However, this task is complicated by other characteristics of water. First, the attenuation of ultrasound in water is much less than body tissues, with the exception of body fluids such as urine or amniotic fluid. Second, waveform distortion due to nonlinear propagation [as in Fig. 1(a)] of the large-amplitude pressure waves encountered in medical ultrasound is much more pronounced in water than soft tissue. These issues notwithstanding, water-based measurements still predominate. However, to estimate the effects of tissue attenuation, so-called *derated* values often are used.

In one common approach for derating water-determined values, it is assumed (1) that a single homogeneous tissue exists between the source transducer and measurement point, and (2) that the attenuation process can be expressed by the following relationship:

$$Q_d = Q_w 10^{-\alpha f_c z} \tag{5}$$

where Q_d is the derated quantity, Q_w is the water-determined quantity, α is the attenuation coefficient, and z is the measurement distance from the source transducer. The most frequently used attenuation is 0.3 dB/cm $\cdot$ MHz^{-1}, which is somewhat less than typical soft tissues. Thus, if Q is pressure, then $\alpha = 0.015$/cm $\cdot$ MHz^{-1}, and if Q is intensity, $\alpha = 0.03$/cm $\cdot$ MHz^{-1}. To denote a quantity derated at 0.3 dB/cm $\cdot$ MHz^{-1}, ".3" is added to the subscript. For example, $I_{SPTA.3}$ is the derated spatial-peak temporal-average intensity.

The effects of finite amplitude distortion can lead to significant underestimates of actual in situ exposure levels using Eq. (5) if the derated calculations are based on large-amplitude measurements in water. Linear extrapolation of small-signal derated fields has been proposed as a solution, but it has been shown that this approach can result in overestimates of the true focal fields. To compensate for these conservatively large values, appropriate correction factors must be derived. For an in-depth discussion of this nontrivial issue, see Ref. 5.

Attenuators and Phantoms. The use of tissue-mimicking attenuators and phantoms also has been studied as a way to avoid the problems associated with determining in situ values from measurements in water. A method has been proposed using attenuators made of low-density polyethylene that are placed between the source transducer and measurement device (6). Also, a phantom for temperature rise measurements comprising thin-film thermocouples embedded in a tissue-mimicking gel has been described (7). Until these methods are standardized, however, water will likely remain the medium of choice for making exposure measurements.

Bioeffects Exposure Indices

The above acoustic quantities have been used to assess the biological effects of ultrasound exposure in two broad categories: thermal, and nonthermal or mechanical. In general the temporal-average quantities have been related to thermal effects, and the temporal-peak and pulse-average quantities to nonthermal effects (principally cavitation). However, both temperature rise and the onset of cavitation are complex functions of the acoustic field and exposed tissue, and none of the above quantities is an adequate indicator of these effects. Therefore, in an attempt to devise more meaningful exposure and dosimetric quantities, the concept of bioeffects indices has been developed. There are two types of indices, a thermal index (TI) and a mechanical index (MI) (the latter sometimes referred to as a cavitation index, or more simply a nonthermal index).

The general definition of the thermal index is the ratio of the measured ultrasonic power (or other power-related parameter) to the ultrasonic power necessary to raise tissue temperature by 1°C. This definition obviously depends on the type of tissue exposed, and to date three TIs have been defined; a soft-tissue thermal index (TIS), a bone-at-focus thermal index (TIB), and a bone-at-surface or cranial thermal index (TIC). The specific formulae for these indices involve combinations of the measurement quantities described above.

The mechanical index is defined as the derated peak rarefactional pressure at the point where the derated pulse intensity integral is a maximum, divided by the square root of the center frequency, or $\mathrm{MI} = p_{r.3}/(f_c)^{0.5}$. The denominator attempts to reflect the observed frequency dependence of the cavitation threshold. The units for pressure and frequency are MPa and MHz, respectively.

See BIOLOGICAL EFFECTS OF ULTRASOUND for further discussion.

MEASUREMENT OF PRESSURE

Piezoelectric Hydrophone

Piezoelectric hydrophones are the most common instruments for measuring acoustic pressure. These devices use a piezoelectric material as a sensing element to convert the mechanical energy in the wave traveling through a medium into an electrical signal whose amplitude is proportional to the pressure. Although in principle these devices can be made from any piezoelectric material, at present piezoelectric polymer elements such as polyvinylidene fluoride (PVDF) are preferred for precise field measurements at frequencies above approximately 100 kHz, the range of most medical applications. This is because the polymer's bandwidth, dynamic range, linearity, and uniformity of frequency response are superior to those achievable with piezoelectric ceramic materials. [Below 100 kHz, where ultrasonic surgical systems that employ vibrating metal tips operate, piezoceramic hydrophones are used (8,9).]

Currently two basic designs of PVDF hydrophones are being used: the needle type and the spot-poled membrane design. Figure 2 shows the design principle for each configuration.

Needle-type Design. The needle-type PVDF hydrophone [Fig. 2(a)] consists of a circular piece of thin (<25 μm), metal-coated PVDF film, typically 0.1 to 1.0 mm in diameter, attached to an insulating layer at the end of a hollow-wall, metal tube. The backing material behind the element has a higher acoustic impedance than water, and, as a result, the resonance corresponds roughly to a quarter-wavelength thickness of the PVDF film. (For backing materials with a very large acoustic impedance, the thickness-resonance frequency, f_r, is approximately $c/4x$, where c is the speed of sound in the PVDF and x is the film thickness). Because the physical dimensions of the needle are very close to the dimensions of the active sensor element, the disturbance of the acoustic field is minimized. Therefore, this construction is particularly useful for spatial field recording and near field, continuous wave (CW) measurements. (In a variation of the needle hydrophone, sometimes called the "baffle" design, the tube or similar structure to which the active polymer element is attached is significantly larger than the film dimensions, but other design aspects are similar.)

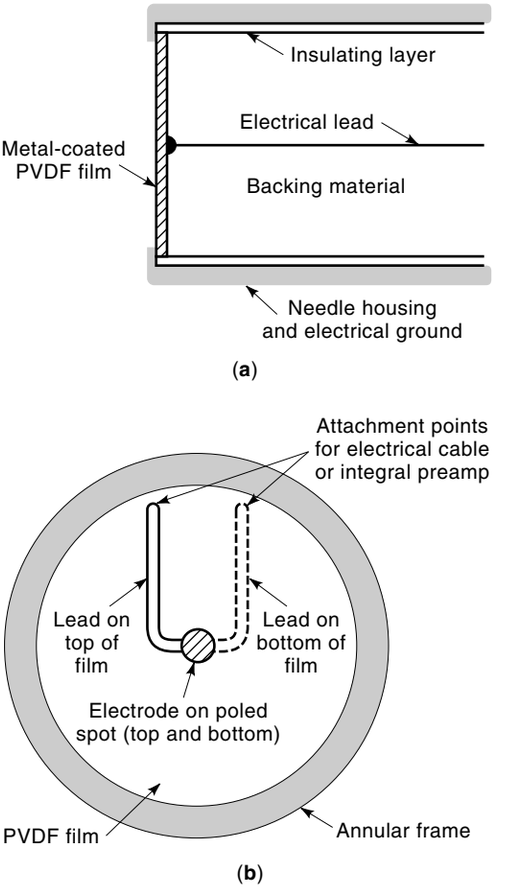

Figure 2. Essential features of polymer hydrophones. (a) Cross-sectional view of tip of needle-type hydrophone; (b) top view of single-layer spot-poled membrane hydrophone showing one of several electrode and lead geometries used. Electrode and lead sizes are exaggerated for clarity.

Spot-Poled Membrane Design. In the spot-poled membrane approach [Fig. 2(b)] a thin (<25 μm) PVDF film is stretched taut across an annular frame usually 5 cm to 10 cm in diameter. Only a small, central portion of the PVDF film is made

piezoelectrically active (spot-poling). Arrays of sensitive elements have been fabricated, but at present a hydrophone with a single spot-poled element is most often used. The sensitive element diameter of current hydrophones, both commercial and experimental, ranges from 0.1 mm to 1 mm. Electrodes and electrical leads are vacuum deposited on the film. These thin films, together with PVDFs relatively low acoustic impedance, enables membrane hydrophones to be highly transparent to sound waves in the medical ultrasonics frequency range (up to 20 MHz). For a sensor operating in a half-wavelength thickness mode (as is the case for the membrane configuration), the thickness-resonance frequency is $f_r = c/2x$. For 4 μm film, the thinnest reported to date (10), this corresponds to a thickness resonance of over 200 MHz.

Sensitivity. The simplest hydrophone consists of the sensitive element, the mounting structure (needle or annular frame) with electrical contacts, and attached coaxial electrical cable. The hydrophone sensitivity M in volts per pascal (V/Pa) for this arrangement can be expressed as

$$M = \frac{V_h}{P_i} = \frac{V_t C_t}{P_i C_T} \tag{6}$$

where V_h is the hydrophone voltage at the end of the cable (connected to an amplifier with known input impedance), P_i is the incident pressure, V_t and C_t are respectively the open-circuit voltage and electrical capacitance of the sensitive element, and C_T is the total capacitance (i.e., the sum of the element, electrical lead, cable, and amplifier input capacitances). Thus, for a given element size, maximizing M involves minimizing C_T. Because the cable capacitance usually predominates, increasing M can be accomplished most easily by locating the hydrophone amplifier closer to the hydrophone housing. This shortening of the cable has the added advantage that the cable resonances excited by high frequency components that can arise from nonlinear distortion of the wave in water are eliminated. Often the hydrophone amplifier is connected directly to or made an integral part of the hydrophone housing [see Fig. 2(b)].

In spot-poled membrane hydrophones the electrical leads that lie on the membrane itself can be a source of signal loss due to capacitive loading. Furthermore, since the capacitance of the leads is a function of the electrical properties of the surrounding fluid, M is medium dependent. This latter problem can be corrected by using a bilaminar membrane design, in which two identical spot-poled sheets such as in Fig. 2(b) are glued together with the sensitive elements aligned, and the outer surfaces are coated with conductive material and connected to the signal ground. Another important advantage of the bilaminar design is that radio frequency (RF) interference and other noise signals are greatly attenuated.

Frequency Response. For accurate measurement of the broad bandwidth pulses encountered in diagnostic and lithotripsy applications, the hydrophone and any associated amplifier should have a uniform frequency response over a wide range of frequencies. For example, diagnostic pulses propagated in water can have significant spectral content up to seven octaves in the range from 100 kHz to 50 MHz.

The high-frequency response of both needle and membrane hydrophones is determined by the film thickness and backing material. For bilaminar membrane hydrophones, the governing dimension is the combined thickness of the two polymer sheets. The response peaks at approximately the thickness-resonance frequency, f_r, described above, the maximum response being approximately 3 dB to 6 dB greater than the flatter region of the response below resonance. The frequency response of the hydrophone amplifier can be designed to compensate for this resonance peak to some extent.

For membrane hydrophones, the response below resonance is smooth and generally uniform to very low frequencies, the lower roll-off being controlled by the $R_a C_T$ time constant, where R_a is the input resistance of the hydrophone amplifier. The low-frequency response of needle hydrophones is more complicated. Fluctuations of several decibels in the response between 1 MHz and 4 MHz are seen due to resonances and reverberations arising in the hydrophone housing. Also, below approximately 1 MHz, a roll-off in the response occurs due to diffraction effects around the needle tip (11).

Effective Size. The hydrophone voltage output is proportional to the spatial integral of the pressure over its active surface. If the hydrophone is not sufficiently small compared to the acoustic wavelength and beam dimensions, then the spatial averaging that occurs will lead to an undermeasurement of the maximum pressure at the point where the hydrophone is located. To avoid spatial averaging errors in practice, the largest effective dimension of the hydrophone's sensitive element (as opposed to its geometrical or physical dimension) should be less than $0.5\ \lambda z/d_s$, where λ is the acoustic wavelength, z is the source-to-hydrophone distance, and d_s is the greatest dimension of the source transducer.

A hydrophone's effective diameter, d_e, is found from a measurement of its directional or angular response to an incident sound field. The response relative to normal incidence is computed and compared to the theoretical angular response of a uniform circular receiver, from which d_e can be calculated.

It is possible to construct a needle hydrophone such that the measured directional response and effective diameter are in good agreement with those predicted by the uniform circular receiver model. However, two features of the spot-poled membrane design can cause significant deviation from this model. One is the presence of accentuated side lobes due to the propagation of membrane (Lamb) waves across the PVDF film when the ultrasound is incident at a critical angle of approximately 50°. At low megahertz frequencies (<2 MHz) these side lobes can be quite large, but the large angles involved usually pose no practical difficulty. The second feature is nonuniform sensitivity over the hydrophone's active element. This nonuniformity can result from the directional dependence of the piezoelectric sensitivity in PVDF, and to fringing effects of the electrical field used to pole the sensitive region of the polymer film. Both effects result in the effective hydrophone size being larger than the physical size of the vacuum-deposited electrodes. Also, the effective size, as compared to that of a uniform circular receiver, is frequency dependent. An approximate expression that relates the effective and physical diameters for spot-poled membrane hydrophones is $d_e(\text{mm}) = [(d_g)^2 + (f)^{-2}]^{1/2}$, where d_g is the geometrical diameter in millimeters and f is the ultrasonic frequency in megahertz.

If $d_e < 0.5\lambda z/d_s$, then details of the directional response are of no concern because spatial averaging is not an issue. How-

ever, for many small-beam, high-frequency diagnostic applications such as ophthalmic, interluminal, interoperative, and small parts, this inequality cannot be satisfied in most cases with current hydrophones. Therefore, spatial averaging correction procedures should be applied to hydrophone measurement results, a relatively unexplored topic. The most promising approach to date (12) involves computing a correction factor δ, which is a function of the nonlinearity propagation parameter σ_m (a measure of the degree of finite amplitude distortion) and a parameter α. This latter parameter (not to be confused with attenuation) is defined as $\alpha = b_{-6}/d_e$, where b_{-6} is the measured -6 dB beamwidth of the quantity being measured, either the peak rarefactional pressure or the pulse intensity integral.

Choice of Hydrophone Type. The choice of a particular hydrophone type depends on the application or given measurement task. Regarding frequency response, the spot-poled membrane design exhibits wider bandwidth due to its pure half-wavelength resonance configuration. The flatter response of the membrane below 1 MHz also may be an important consideration, especially when measuring peak rarefactional pressure amplitudes in nonlinearly distorted waves. This is because the portion of the pressure waveform where p_r occurs is dominated by low-frequency components (13).

Although membrane hydrophones possess a high degree of acoustical transparency, they are more vulnerable to the generation of the standing waves when measuring CW fields. Therefore, needle-type hydrophones are preferable for CW measurements. In addition, because of its large size, the membrane design is not well suited wherever measurements have to be carried out in confined spaces. For in vivo measurements, the classical membrane design is impractical and a needle design or its modification must be used. In this context, it is interesting to note that a seven-element linear array of PVDF elements also has been used to measure in vivo exposures intervaginally during an obstetric ultrasound examination (14). The PVDF elements were positioned near one end of a stainless steel tube. The element size and spacing were 0.5 mm and 1.5 mm, respectively.

The most significant contribution to measurement uncertainty with currently available piezoelectric hydrophones is due to their finite aperture. The membrane's angular response is less predictable than that of a well-designed needle-type hydrophone. Current experience indicates that fabrication of a needle-type hydrophone with a 0.050 mm effective diameter is feasible. A prototype spot-poled membrane hydrophone with an apparent effective diameter of 0.1 mm has been reported (10).

Single-layer membrane hydrophones should only be used in deionized water because of the exposed leads. If deionized water is not available, or if electrical interference is a problem, a bilaminar membrane or needle-type hydrophone is necessary. Lithotripsy devices present a challenging measurement problem because the focused shock waves tend to destroy the hydrophone, primarily by eroding the metal electrodes and leads. One solution is to use a disposable hydrophone, and membrane hydrophones have been designed to this end. Another approach is to construct a membrane hydrophone with electrodes separated from the film and therefore away from the focus, thus forming a capacitively coupled device.

Displacement Sensors

It can be seen from Eq. (3) that, for plane acoustic waves, the pressure amplitude can be calculated from a measurement of the acoustic displacement. Two techniques have been used for this purpose: laser interferometry and capacitance probes.

Interferometer. In this approach a thin membrane (pellicle) is placed in a water tank parallel to the face of the source transducer. If the pellicle is suitably thin, then it can be considered acoustically transparent and flexible enough to move with the water particles in response to the ultrasonic waves. If the side of the pellicle opposite the source transducer is coated with metal to enhance optical reflectivity, then this metal surface can be interrogated with a laser, allowing the displacement of the interrogated spot on the pellicle to be measured interferometrically. That is, the normal component of displacement is determined by comparing the phase of the reflected light beam to that of a reference beam. If the displacement is small compared to the optical wavelength, then the displacement and phase shift are proportional.

Although conceptually straightforward, the design and practical implementation of this technique can be difficult due to several factors, among them the need for isolation from environmental vibrations and determining the frequency response of the optical detection system. With regard to the former, an optical heterodyne process has been reported that makes the measurements of transient fields insensitive to environmental disturbances such as low-frequency motions of water (15). For 3 μm thick pellicles, bandwidths of 30 MHz are possible. Spatial and temporal resolutions of 0.02 mm and 0.01 μs, respectively, have been achieved.

Capacitance Probe. Acoustic displacement detection also can be accomplished by monitoring ultrasonically induced changes in the gap width of a parallel-plate, air-dielectric capacitor. To implement this scheme, the ultrasonic waves traveling in water are made to strike the front surface of the metal plate, which plate forms one surface of the capacitor. A portion of the transmitted waves is reflected at the back surface, modulating the air cavity and causing a change in the capacitance. The thickness of the front plate must be large enough ($\gtrsim$10 mm) so that errors caused by internal reflections and flexural vibrations are minimized.

The method provides an absolute measurement of displacement, and it has a wide frequency response. Also, the transducer is robust. However, practical effective acoustic dimensions of less than a few millimeters are difficult to achieve, which makes the device useful primarily for lithotripsy applications, where spatial resolution is not as critical, and where its durability is a key feature.

Fiber-Optic Sensor

Sensors made from optical fibers can be configured to respond to a wide range of physical quantities, including acoustic pressure. Because these flexible light pipes can be obtained in small diameters and are robust and immune to electromagnetic interference, they have advantages in the measurement of medical ultrasound fields, particularly for lithotripters.

Two configurations have been explored for measurements at medical frequencies. In the first, the end of a glass or polymer fiber is oriented in the ultrasonic beam as one would a

needle-type hydrophone. The intensity of light reflected from the fiber endface follows the temporal variations in the local acoustic pressure because of changes in the density-dependent refractive indices of the fiber and water. This technique has been used primarily for lithotripter studies, because the minimum detectable pressure is greater than that of polymer hydrophones. For example, a device with a 0.1 mm fiber diameter, 20 MHz bandwidth (limited by the photodetector amplifier), and minimum detectable pressure of 1 MPa has been reported (16). One advantage of this device is that if the fiber tip eventually is damaged by the lithotripter pulses, the fiber need only be cut to produce a new tip. For lower pressure applications, future refinements such as coating the endface with an appropriate material may result in improved sensitivity.

In the second configuration, a polarization-maintaining fiber is oriented perpendicular to the ultrasound beam axis. This type of optical fiber has an anisotropic refractive index. That is, the fiber can be regarded as an intrinsic birefringent medium with two orthogonal principal axes. Thus, light waves linearly polarized along these two axes propagate at different velocities. When the length of the fiber is subjected to an acoustic disturbance, it is possible to detect a phase difference between the two polarized light beams. This ultrasonically induced phase change, and the subsequent change in light intensity at the far end of the fiber, is proportional to the line integral of the instantaneous acoustic pressure along the fiber.

This approach, with 80 μm to 125 μm diameter fibers, has been used for measurements of diagnostic-like fields as well as high-power hyperthermia transducers. Because the photodetector output is proportional to the line integral of the pressure, tomographic reconstructions have been performed to compute the pressure distributions on planes normal to the beam axis. The advantages of this technique are its improved sensitivity, low susceptibility to damage in intense ultrasound fields, immunity to electrical interference, and good spatial resolution. However, determining the pressure amplitudes is computationally demanding, and the method does not yield temporal "point" pressure waveforms. Also, because the device is a line sensor, phase cancellations can result from misalignment of the fiber or from nonplanar wavefronts, and phase distortion occurs due to frequency-dependent time-delays in the fiber.

Acousto-optic Diffraction

Ultrasonic pressure waves produce a periodic change in the density of the medium in which they propagate, which causes small fluctuations in the optical refractive index for transparent media. A beam of light passing through these local inhomogenities will experience slight velocity (and phase) deviations, the amount dependent among other things on the ultrasonic frequency, pressure amplitude, and interaction angle. This interaction of light and sound is the basis for so-called acousto-optic diffraction measurements, in which it is assumed that the ultrasound beam acts as an optical phase grating to a beam of light normally incident to the direction of sound propagation. With suitable optics, this grating can cause a monochromatic light source passing through the sound beam to produce a linear pattern of dots known as a Fraunhofer diffraction pattern. The central dot is the direct, undiffracted light from the source, and the adjacent dots represent light diffracted by the ultrasound.

If the central dot is blocked so that only light diffracted by the ultrasound is passed, this diffracted light can be projected on a screen to give a side visualization of the sound beam. Within certain acoustic pressure limits, the brighter the optical image, the greater the relative pressure of the sound field at that corresponding location. This so-called schlieren technique has been used for qualitative views of both therapy and diagnostic sound beams. For pulsed fields, the light and ultrasound beams must be synchronized.

In more quantitative terms, the light intensity (I_n) in each of the successive dots, or diffraction orders (n), is proportional to $[J_n(\nu)]^2$, where J_n is the nth order Bessel function, and ν represents the maximum optical phase shift. This phase shift can be expressed as,

$$\nu = k\kappa \int p\, dl \tag{7}$$

where k is the optical wave number, κ is the adiabatic piezooptic coefficient (Pa^{-1}), and p is the acoustic pressure (Pa), which is integrated over the path of interaction of the light and sound.

If, by appropriate spatial filtering, only the light in the first order (J_1) is detected, and if $\nu \ll 1$ (the so-called Raman–Nath regime), then $J_1(\nu)$ is approximately proportional to ν, and the light intensity is proportional to the square of the line integral of the pressure, or

$$(I_1)^{0.5} \propto \int p\, dl \tag{8}$$

Because Eq. (8) contains the integral of the pressure, tomographic reconstruction is necessary (as was the case with one of the fiber-optic devices) to create two-dimensional distributions of the pressure amplitude. Furthermore, outside the Raman-Nath regime the use of Eq. (8) becomes more questionable, a consideration that applies to lithotripter and some of the higher output therapy and diagnostic applications. In these large amplitude cases useful schlieren images have been made using the higher orders of diffracted light, but the relationship between light intensity and pressure is less perspicuous.

Major advantages of this technique are its ability to provide rapid two-dimensional beam plots, its inherently nonperturbing nature, and good spatial resolution. One compact system consisting of an infrared laser and charge-coupled device (CCD) camera for recording the images has been used for making quantitative beam measurements (17). This system has a reported spatial resolution of 50 μm. Also, by integrating the square of the reconstructed pressure distribution [see Eq. (2)], the temporal-average ultrasonic power has been obtained with this system. (Other power measurement methods are discussed in a later section.)

MEASUREMENT OF INTENSITY

Intensity Derived from Hydrophone Measurements

Under the conditions for which Eq. (2) is valid (plane or spherical progressive waves), the hydrophone sensitivity M in Eq. (6) can be used to derive the intensity from the hydrophone-measured pressure. If $v_h(t)$ is the hydrophone volt-

age, then

$$i(\mathrm{t}) = [v_{\mathrm{h}}(t)]^2/M^2\rho c \tag{9}$$

For intensity units of W/cm^2 and units for M of V/MPa (both commonly used), $i(t) = 67[v_{\mathrm{h}}(t)/M]^2$ in water ($\rho c = 1.5 \times 10^6$ Ns/m^3). Obviously, Eq. (2) could be used to calculate the intensity from any of the other methods described for obtaining the acoustic pressure as well.

Suspended-Sphere Radiometer

If a beam of ultrasound is incident on an obstacle or target that either reflects or absorbs the energy in the beam, then momentum is transferred to that target. This momentum can be measured as a radiation force that is proportional to the temporal-average intensity in the beam. If the target intercepts the entire beam, then the force yields the total ultrasonic power. If the target is small compared with the beam dimensions, then the force provides a measure of the local intensity.

The suspended sphere radiometer is an example of a small-target radiation force device. The reflecting target is a spherical metal ball no greater than several wavelengths in diameter that is suspended vertically in the horizontally directed sound field via a thin filament. For small angle deflections, the spatial-peak temporal-average intensity can be computed as

$$I_{\mathrm{SPTA}} = mg\,dc/L\pi a^2 Y \tag{10}$$

where m is the effective mass of the ball (corrected for buoyancy), g is the gravitational constant, d is the horizontal deflection of the sphere due to the radiation force, c is the speed of sound in the medium (usually degassed, distilled water), L is the filament length, a is the radius of the sphere, and Y is a dimensionless quantity known as the acoustic radiation force function. The deflection can be measured with a traveling microscope. Y depends on the ratio of the ball diameter to the wavelength in the medium, the medium density, and the elastic properties of the ball. The technique has been used in the frequency range 0.25 MHz to 10 MHz. However, because Y is a complicated function of the wavelength, practical use of this technique is restricted to narrow bandwidth or continuous-wave fields. Also, errors can arise from acoustic streaming, particularly when nonlinear propagation increases the effective transfer of momentum from sound beam to water. Acoustic intensities of from 10 mW/cm^2 to 10 W/cm^2 have been measured.

Thermoelectric Sensor

As ultrasound propagates, a decrease in the wave amplitude with distance can occur through two attenuation mechanisms: absorption and scattering. Absorption, which is due to such factors as viscous effects and molecular relaxation, results in the conversion of a portion of the wave energy into heat. For plane-wave propagation, this local production of heat can be expressed quantitatively as $q = \alpha I_{\mathrm{TA}}$, where q is the average rate of heat generation per unit volume per unit time (J/m$^3 \cdot$ s^{-1}), α is the intensity absorption coefficient per unit length (per meter) [see Eq. (5)], and I_{TA} is the local temporal-average intensity (W/m^2). Furthermore, where conduction or other heat-loss mechanisms can be neglected, the local rate of temperature rise is given by $dT/dt = q/C_{\mathrm{h}}$, where C_{h} is the heat capacity per unit volume (J/°C $\cdot$ m^{-3}). Combining these two equations gives the following relationship between the ultrasonic intensity and temperature in a sound-absorbing medium:

$$I_{\mathrm{TA}} = (C_{\mathrm{h}}/\alpha)\,dT/dt \tag{11}$$

Equation (11) has been used as the basis for measuring intensity by enclosing (i.e., embedding or coating) a small thermoelectric sensor in a suitable absorbing medium and then measuring the slope of the ultrasonically induced temperature versus time curve. This process assumes that the values of C_{h} and α have been determined, but it also is possible to calibrate the probe by other means such as the suspended-sphere radiometer, a procedure always done for coated sensors.

In practice both thermocouples and thermistors have been used. Their presence affects the initial temperature rise due to viscous effects at the sensor surface, resulting in a rapid initial temperature increase followed by a more gradual rise. I_{TA} has been calculated using Eq. (11) by measuring dT/dt during this second phase of the sensor response, which occurs roughly between a few tenths and one second after insonation. To avoid heat loss effects (mainly conduction) over this time, temperature gradients must be minimized, which places restrictions on the minimum ultrasound beamwidth, as well as the dimensions and conductivity of the embedding material and sensor leads. To make the measurement less sensitive to conduction effects, the initial, more rapid increase in temperature rise also can be used to measure intensity. In this case an independent calibration of sensor response is necessary.

A thermoelectric sensor can be fabricated with an extremely small measurement volume, so very good spatial resolution can be achieved. Sensor elements as small as 1 μm are possible (but field perturbation by coatings and electrical leads still must be considered). Minimum detectable values of I_{TA} for some devices have been no better than a few hundred milliwatts per square centimeter. However, with proper selection of sensor and embedding or coating materials, intensity measurements on the order of a few milliwatts per square centimeter have been realized in other instances.

Poor temporal resolution (several tenths of a second) restricts the technique to temporal-average measurements. Also, since α is frequency dependent, the technique is best applied to CW or long pulse measurements. For these reasons thermoelectric sensors are most useful for exposure measurements in therapeutic and some diagnostic Doppler applications. Also, as noted earlier, these sensors are finding use in dosimetric studies of temperature rise in tissue-mimicking phantoms (7).

MEASUREMENT OF POWER

Radiation Force Devices

In the discussion of the suspended sphere radiometer it was stated that if the perfectly reflecting or absorbing target intercepts the entire ultrasonic beam, then the radiation force yields the total temporal-average ultrasonic power. The force F acting in the direction of propagation of the acoustic wave can be expressed as $F = (2W\cos^2\theta)/c$ for a reflecting target and $F = W/c$ for a totally absorbing target, where W is the

temporal-average power in watts, θ is the angle of incidence measured from normal, and c is the speed of sound in water in m/s. If $\theta = 45°$ for a reflecting target or any angle for an absorbing target, $F/W = 67$ mg/W.

Devices that measure the radiation force represent an important type of measurement instrument because of their convenience in determining the ultrasonic power. Many different designs have been developed, depending on requirements regarding sensitivity, dynamic range, and portability. As an example, consider the diagram of a radiation force balance shown in Fig. 3. This device, often found in a laboratory setting, uses a standard analytical balance or more sophisticated feedback-based null detector to achieve the required sensitivity for measuring the low power levels found in some diagnostic applications. The target is an air-backed conical reflector suspended in the water tank with thin filaments. The cone angle is 45°. The balance responds to the radiation force produced by the source transducer under test with an apparent change in the weight of the target. The tank is lined with acoustic absorbing material such as rubber to minimize reflections and standing waves.

In radiation force devices designed to measure powers above approximately 1 W, the water should be degassed to prevent the formation of bubbles that could reflect the sound before it reaches the target. For ultrasonic frequencies above 5 MHz, results should be corrected for the attenuation of the water. When finite amplitude distortion is expected, the source-to-target separation should be kept small to minimize the generation of harmonics. Also, often a thin, acoustically transparent membrane separating the target and source transducer is used to minimize errors due to the phenomena of acoustic streaming.

In Fig. 3 a reflecting target is shown. Absorbing targets are used as well in some devices because there is no angle dependence. However, perfectly absorbing wideband target materials are not easily available. In addition, in the diagnostic range of frequencies, say, 2 MHz to 20 MHz, the information on absorbing characteristics of different target materials is largely lacking. Absorbing targets also can create standing waves due to the imperfect absorption of acoustic energy, and they can cause temperature drifts in the balance system due to the energy absorption.

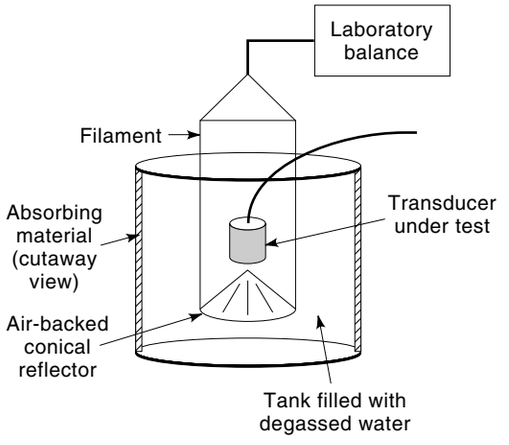

Figure 3. Diagram of laboratory radiation force balance for measuring ultrasonic power.

Uncertainties of approximately ±10% are achievable with well-designed radiation force balances.

Calorimeter

Calorimetric devices are based on measurement of the heat generated when the energy in an ultrasound beam is totally absorbed. Two measurement procedures can be distinguished: direct and comparison. In the direct procedure the temporal-average ultrasonic power is determined from a temperature rise measurement, given the heat capacity of the absorbing material and other system characteristics. Because a complete thermal analysis of the system is difficult, the direct method suffers relatively high overall uncertainties. These uncertainties can be minimized by employing the comparison method. Here, two identical absorption chambers are used. An electric heating device produces a temperature elevation in one chamber equal to that generated by the measured ultrasound beam in the other. Once the temperatures are brought to the same level, the value of ultrasonic power is determined by measurement of the corresponding electrical power.

Both flow and nonflow calorimeters have been used. In the flow calorimeter a liquid (e.g., distilled water, or a more absorbent liquid such as carbon tetrachloride or a perfluorinated hydrocarbon) is continuously circulated through the calorimeter and the ultrasonic power is determined from the measurement of the temperature difference between the outflow and the inflow ports. In the nonflow (constant mass) calorimeter the absorbing medium is contained within the measurement vessel and the source transducer is turned on for a limited period of time only. In this approach the power is determined by measurement of the rate of the temperature increase.

One of the main problems with calorimetric measurements of ultrasonic power is to separate the heat generated internally by the source transducer, due to its electromechanical conversion inefficiency, from that due to the absorption of the acoustic energy. This problem can be overcome by designing a water flow system between the source transducer face and the absorbing chamber to carry away the unwanted heat.

Calorimeters have been designed for use over the power range 1 mW to 10 W. Measurements typically take several minutes to complete, and an uncertainty of less than ±10% over the frequency range of 1 MHz to 15 MHz is achievable. The calorimetric approach has the advantage that it is independent of acoustic field characteristics such as pulse duration, beam shape, and nonlinear propagation phenomena, and it does not require the assumption of plane wave propagation. However, set-up and operation can be difficult, so it is used much less frequently for measuring power than radiation force techniques.

Planar Scanning

Equation (4) can be used to compute the ultrasonic power by scanning a hydrophone over the surface S and computing the temporal-average intensity at points r, $I_{TA}(r)$, from the measured hydrophone voltages. Implicit in this approach is that Eq. (2) is valid. With

$$I_{TA}(r) = \frac{1}{T}\int_0^T i(t)\,dt \tag{12}$$

Eqs. (2) and (6) can be used to express the power in Eq. (4) as

$$W = \int_S h(r)\, dS/M^2 \rho c \tag{13}$$

Here $h(r)$ has been defined as the temporal-average of the square of the hydrophone voltage,

$$h(r) = \frac{1}{T}\int_0^T [v_h(r,t)]^2\, dt \tag{14}$$

where $v_h(r, t)$ is the instantaneous hydrophone voltage at position r on S, and T is the temporal integration interval, which for pulsed source transducers is usually the pulse repetition period.

Scanning normally is done in a plane at an axial distance from the source transducer where Eq. (2) is valid. The surface integral may be found by performing a series of linear, parallel scans (i.e., raster scans) with the hydrophone. However, for circular source transducers in which cylindrical beam symmetry can be assumed, the surface integral reduces to a line integral along a beam diameter. In practice in this latter case it is prudent to average the results of at least two orthogonal diametric scans, because perfect beam symmetry is rare. Another practical matter concerns the choice of scan limits. In general, the hydrophone should be scanned laterally from the beam center until no ultrasound signal is observed above the noise. In practice, a limit of -26 dB relative to the peak value of $h(r)$ is often used [i.e., 0.25% of maximum $h(r)$]. In this regard, measurement accuracy decreases in beams having a significant fraction of the total power in the low level skirts of the beam that occupy much greater area than the main lobe.

The distance between hydrophone steps and scan lines depends on the beam size and hydrophone effective diameter. Regarding the latter, correction for spatial averaging effects (12), as well as hydrophone directivity, should be made if necessary to avoid systematic errors associated with the finite aperture of the hydrophone. The scans typically are made in a water-filled tank lined with acoustic absorbing material. The water should be degassed to avoid the formation of gas films or bubbles on the source transducer, hydrophone, or absorbing materials, and it should be deionized if the hydrophone has unshielded leads. For frequencies above about 5 MHz, the attenuation of water should be accounted for in the calculation. Maximum uncertainties for determining ultrasonic power via the planar scanning technique increase from approximately $\pm 10\%$ to $\pm 20\%$ as the frequency is changed from 1 MHz to 15 MHz.

The planar scanning technique is slow compared to the radiation force or calorimetric techniques. It also is limited in practice to stationary (nonscanning) beams. However, it has the advantage that it also results in beam plots of the pressure or intensity distribution in the plane of measurement, which can be useful in assessing the fine structure of the beam and in determining beam areas and widths.

HYDROPHONE CALIBRATION

Several methods have been used to determine the hydrophone sensitivity M in Eq. (6). These methods also would be applicable to the calibration of other pressure-sensing devices, such as the first fiber-optic probe configuration described earlier.

Planar Scanning

Equation (13) describes a way to measure the ultrasonic power via a scanning hydrophone if the hydrophone sensitivity M is known. However, if the power had been determined by another method (e.g., radiation force), then M could be calculated from

$$M = \left[\int_S h(r)\, dS/W\rho c\right]^{0.5} \tag{15}$$

The source transducer usually is excited at a single frequency. Therefore, to find the frequency dependence of M, the planar scanning procedure would have to be repeated at each frequency, which is a fundamental limitation of this technique. However, if the relative frequency response of the hydrophone is known, then planar scanning can be a convenient way to establish the absolute broadband sensitivity, since a hydrophone scanning system usually is an integral part of an ultrasound measurement laboratory.

Interferometer

The technique of laser interferometry described previously can provide an absolute and accurate measurement of acoustic displacement, and it has found use in national ultrasound standards laboratories for hydrophone calibration purposes. In this method a substitution technique is employed; that is, after a measurement of the displacement and calculation of the pressure amplitude via Eq. (3), the hydrophone is placed at the point in the ultrasound field where the laser was reflected from the pellicle.

In addition to the vibration and frequency response problems mentioned earlier, a number of other factors must be dealt with in performing the calibration. For instance, in the region between the pellicle and laser source the laser and sound beams coincide. Thus, the calibration involves correcting for the effect that the sound beam has on the index of refraction of water. Also, since the light beam is smaller than the effective diameter of most hydrophones, spatial averaging effects must be considered. Properly executed, however, the technique is very accurate, with uncertainties of 2.3% to 6.6% being reported over the frequency range 0.5 MHz to 15 MHz.

Reciprocity

Reciprocity methods employ at least one reciprocal transducer, that is, a transducer that can be used as both transmitter and receiver, and that satisfies certain additional conditions such as being linear and passive. For such a transducer the receiving voltage sensitivity M (transducer voltage output per pressure input) divided by the transmitting current response S (pressure transmitted per transducer current input) is equal to a quantity called the reciprocity parameter J, which is a function of the propagation medium, frequency, and transducer geometry. The reciprocity procedure used almost exclusively in the ultrasonic frequency range (above 500 kHz) for hydrophone calibration is called the two-transducer reciprocity method, the two transducers being the hydrophone under test and a so-called auxiliary transducer. This calibra-

tion method yields the absolute hydrophone sensitivity at a particular excitation frequency from a measurement of the transducer current, voltage, and frequency.

The experimental arrangement is shown in Fig. 4. The auxiliary transducer, having transmitting and receiving responses S_A and M_A, respectively, is excited with a sinusoidal current burst I_1, which produces pressure pulse P_1. The pressure returned from a planar reflector produces voltage V_1. With $S_A = P_1/I_1$, $M_A = V_1/P_1$, and $M_A/S_A = J_p$, the transmitting response can be computed as $S_A = (V_1/I_1J_p)^{0.5}$. For this configuration J_p denotes the plane-wave reciprocity parameter, which is given by $2A/\rho c$, where A is the effective radiating area of the transmitter, and ρ and c are the density and the speed of sound in the medium (water), respectively.

Subsequently, the reflector is tilted slightly ($<15°$) such that the hydrophone to be calibrated is on the axis of the reflected sound field, at the same distance from the reflector as the auxiliary transducer. Exciting the auxiliary transducer with current I_2 (not necessarily equal to I_1) produces pressure P_2, which in turn results in hydrophone voltage V_h. With $P_2 = S_AI_2$, the sensitivity of the hydrophone can be determined from

$$M_h = V_h/P_2 = (V_h/I_2)(I_1J_p/V_1)^{0.5}\text{V/Pa} \tag{16}$$

Although conceptually simple, execution is nontrivial because alignment of the transducers and reflector is critical, and because Eq. (16) assumes ideal measurement conditions such as perfect sound reflection, open-circuit transducer operation, a lossless medium, and plane-wave propagation (i.e., no errors due to diffraction). To compensate for these effects, complicated correction factors must be introduced. When all the correction factors are taken into account, and assuming that the voltage and current can be measured to within $\pm 2\%$, the estimated overall maximum uncertainty is $\pm 18\%$ in the frequency range 1 MHz to 15 MHz.

Time Delay Spectrometry

The three previous hydrophone calibration procedures, planar scanning, interferometry, and reciprocity, are all discrete frequency techniques. Therefore, obtaining the hydrophone sensitivity as a function of frequency entails time-consuming point-by-point measurements. A more efficient method makes use of the swept-frequency technique know as time delay spectrometry (TDS).

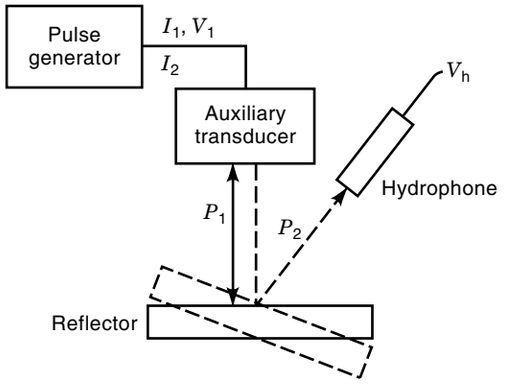

Figure 4. Diagram for reciprocity calibration of a hydrophone.

In TDS a source transducer of suitable bandwidth is excited with a sinusoidal signal that is swept linearly between frequencies f_1 and f_2. The frequency sweep rate, s, is F/T_s, where $F = f_2 - f_1$ and T_s is the sweep time. The hydrophone under test is placed a distance d from the source transducer, and its voltage signal is fed to a narrow-bandpass tracking filter. This filter also sweeps over F at rate s, but the sweep is delayed in time by the propagation delay between the source and hydrophone, that is, by $t_o = d/c$, where t_o is the time delay and c is the speed of sound in the propagation medium (usually distilled, deionized water). The difference in frequency (frequency offset), Δf, between the transmitted signal and the filtered hydrophone signal is $\Delta f = t_o s$. Because the tracking filter sweeps in synchrony with but at a constant frequency offset from the source, only signals traveling directly from the source to the hydrophone will be detected. All reflected signals, whether from the water surface, water tank walls, or structures in the tank, will be filtered from the hydrophone signal. Thus, in addition to providing an efficient means for measurements over a range of frequencies, the technique is highly immune to multipath interference, and it can effectively allow free-field measurements in a highly reflective environment. Also, because of the narrowband filtering, the signal-to-noise ratio (SNR) is very high, so problems associated with finite amplitude distortion in water can be avoided by the use of relatively low acoustic pressures.

The spatial resolution of the TDS system, that is, the minimum allowable pathlength difference between direct and reflected paths, is cB/s, where B is the tracking filter bandwidth. Inherently, the frequency resolution varies inversely with the temporal (and therefore spatial) resolution. The choice of B, which determines the frequency resolution, depends on such factors as the sweep rate, filter transient response, and desired SNR. A useful criterion is $B^2 \geq s$. In practice, the combination of bandwidth and sweep rate can be selected so as to detect the sharp amplitude fluctuations that sometimes occur in the frequency response of needle-type hydrophones due to spurious mechanical or radial mode resonances.

Realizing the full potential of the TDS technique requires using a source transducer with a bandwidth broad enough to cover the frequencies of interest. If such a transducer cannot be found or fabricated, it is possible to overlap the results of several transducers that have more restricted frequency ranges. Also, TDS is not an absolute method, but it can be used in combination with two-transducer reciprocity to provide an absolute hydrophone calibration as a nearly continuous function of frequency. Alternatively, if a previously calibrated (i.e., reference) hydrophone is available, then a substitution calibration can be performed by comparing the TDS measurement of the reference hydrophone to that of the hydrophone under test.

Broadband Pulse

In the above calibrations methods, either single-frequency or swept sine waves are used to energize the source transducer. As an alternative approach, if a broadband pressure pulse $p_i(t)$ having known spectral content $P_i(f)$ could be produced, then the hydrophone sensitivity as a function of frequency, $M(f)$, could be found in a single measurement from

$$M(f) = V_h(f)/P_i(f) \tag{17}$$

where $V_h(f)$ is the voltage spectrum of measured hydrophone voltage $v_h(t)$ [see Eq. (6)].

Such an approach is possible if a thick piezoelectric source transducer is used. *Thick* in this context means that the duration of the electrical signal exciting the transducer is short compared to the acoustic propagation time through the transducer. Let this propagation time be t_T, and let the transducer excitation pulse be $v(t)$ with spectrum $V(f)$. Furthermore, consider a hydrophone located on the beam axis at axial distance z in water with sound speed c. If the source is excited at time $t = 0$, then transducer theory states that for times $t < z/c + t_T$ the radiated field directly in front of and close to the source transducer consists solely of a plane-wave pressure pulse $p(t)$ such that, above some lower frequency limit f_m, $P(f)$ is proportional to $V(f)$ (18). Equation (17) then would become,

$$M(f) = V_h(f)/KV(f), \quad f > f_m \tag{18}$$

The hydrophone distance z must be small enough so that other radiation effects due to the finite aperture of the source transducer (so-called edge and head waves) arrive at the hydrophone after time $z/c + t_T$. In practice this is not a practical limitation.

The values of K and f_m depend on the piezoelectric and dielectric properties of the source transducer material, the acoustic impedances of the transducer and propagation medium (water), and the source transducer thickness. Rather than calculating K and measuring $v(t)$, $p(t)$ can be determined from a measurement of the displacement of the front face of the source transducer, $\xi(t)$, via laser interferometry in a manner similar to that discussed previously. Then, $p(t) = \rho c d\xi(t)/dt$ [see Eq. (3)]. In this approach some measurement problems can be avoided if the source transducer is directed vertically upward toward the water surface, which then acts as the pellicle, and the laser path is entirely in air. Also, if a hydrophone with known frequency response is available, then a substitution calibration can be performed as described previously.

Advantages of this technique are its ability to provide broadband calibration data in a single measurement, and the lack of a need for precise source-hydrophone positioning. However, sensitivity is poor, because the source transducer is neither focused nor operated in a resonant mode. Also, for practical source transducer dimensions (e.g., a 2.54 cm thick piezoceramic disk having a 6 cm diameter), the frequency limit for f_m is about 200 kHz, which is acceptable for most, but not all, medical ultrasound applications.

Substitution in a Nonlinear Field

Another technique for calibrating over a wide frequency range in a single measurement uses a broadband ultrasonic field produced by nonlinear propagation. Calibrations are done at the fundamental excitation frequency and all harmonic frequencies, the number of harmonics determined by the degree of nonlinear distortion in the wave. In practice, a 1 MHz source transducer can produce useful harmonics to at least 20 MHz.

Calibration is performed via substitution. A reference hydrophone having a known frequency response is placed in the nonlinear field, then the hydrophone to be calibrated is placed at the same location, and the two output voltages are compared. The frequency resolution is inherently limited to the fundamental excitation frequency, but this is not a severe restriction for polymer needle hydrophones above a few megahertz, or for spot-poled membrane hydrophones.

MEASUREMENT AND CALIBRATION STANDARDS

International Standards

The group that has been the most instrumental in the development of international standards related to the characterization of medical ultrasound fields, as well as the calibration of measurement devices, is the International Electrotechnical Commission (IEC), an organization responsible for international standardization in the electrical and electronics field. Within the IEC, Technical Committee 87: Ultrasonics (TC87) has produced six notable standards to date, and it is actively pursuing a number of others. These standards are described briefly below.

IEC 866—*Characteristics and calibration of hydrophones for operation in the frequency range 0.5–15 MHz (1987).* This standard covers the design and performance requirements of hydrophones employing piezoelectric sensor elements that are designed to measure pulsed and CW ultrasonic fields. Also described is the two-transducer reciprocity method for hydrophone calibration.

IEC 1101—*The absolute calibration of hydrophones using the planar scanning technique in the frequency range 0.5–15 MHz (1991).* Another method described above for hydrophone calibration, the planar scanning technique using an ultrasonic source transducer of known power, is specified in this standard. The accuracy is comparable with that of the reciprocity method.

IEC 1102—*Measurement and characterization of ultrasonic fields using hydrophones in the frequency range 0.5–15 MHz (1991).* The objectives of this standard include defining a group of acoustic exposure parameters that can be measured on a physically sound basis, and specifying the conditions under which these parameters can be measured using hydrophones. Acoustic pressure is the primary measurement quantity, and various derived intensity parameters are defined under certain assumptions.

IEC 1157—*Requirements for the declaration of the acoustic output of medical diagnostic ultrasound equipment (1992).* This standard specifies the acoustic output exposure information that should be declared by the manufacturers of diagnostic equipment. Three categories of information are to be supplied by manufacturers: in technical data sheets for prospective purchasers, in accompanying literature or manuals, and in background information documents requested by interested parties. In all three categories the exposure information is obtained from measurements made in water.

IEC 1161—*Ultrasonic power measurement in liquids in the frequency range 0.5–25 MHz (1992).* Of the several extant approaches for determining the ultrasonic power, this standard concentrates on the radiation force balance method. General principles for the use of this technique are established.

IEC 1689—*Ultrasonics-Physiotherapy systems—Performance requirements and methods of measurement in the frequency range 0.5–5 MHz (1996).* Measurement methods and characterization of the output performance for ultrasound devices used in physical therapy are covered in this standard. It is applicable to equipment employing a single plane circular transducer that generates continuous of quasicontinuous ultrasonic energy.

Other standards being developed by TC87 include measurement and characterization of focusing transducers, measurement of the output characteristics of ultrasonic surgical systems and pressure pulse lithotripters, measurement uncertainty for radiation force balances, hydrophone calibration below 0.5 MHz and above 15 MHz, test objects for determining temperature increase, and test methods for determining thermal and mechanical exposure parameters for the purposes of defining the safety classification of medical ultrasound fields.

National Standards

The United States has been the most active country in developing ultrasound measurement and calibration standards. Two standards relevant to exposimetry and dosimetry for medical diagnostic applications are published jointly by the American Institute of Ultrasound in Medicine (AIUM), an organization that promotes clinical use, research, safety, standards, and education, and the National Electrical Manufacturers Association, a trade association representing most of the diagnostic ultrasound industry. These standards are as follows.

1. *Acoustic Output Measurement Standard for Diagnostic Ultrasound Equipment (1998).* The objectives of this standard are (i) to set forth precise definitions of acoustic quantities, especially as related to acoustic output levels, and (ii) to specify standard measurement procedures for these quantities. Measurements are to be performed in water; however, derated values are defined and discussed.
2. *Standard for Real-Time Display of Thermal and Mechanical Acoustic Output Indices on Diagnostic Ultrasound Equipment, Rev. 1 (1998).* This standard defines the thermal and mechanical indices (TIB, TIS, TIC, MI), provides a measurement methodology for their determination, and specifies the conditions under which they are to be displayed on the equipment. The goal of this standard is to make device operators aware of the ultrasonic output of their instrument via the real-time display of biologically relevant exposure indices, so that exposures can be minimized easily and effectively, and prudent risk-benefit decisions can be made.

BIBLIOGRAPHY

1. M. C. Ziskin and P. A. Lewin, (eds.), *Ultrasonic Exposimetry,* Boca Raton, FL: CRC Press, 1992.
2. R. C. Preston, (ed.), *Output Measurements for Medical Ultrasound,* London: Springer-Verlag, 1991.
3. G. R. Harris, P. A. Lewin, and R. C. Preston, (eds.), Special Issue on Ultrasonic Exposimetry, *IEEE Trans. Ultrason. Ferroelectr. Freq. Control,* **35**: 85–269, 1988.
4. M. W. Greene, (ed.), *Non-ionizing Radiation—Proc. 2nd Int. Non-Ionizing Radiation Workshop* Section III, Ultrasound, p. 125–224, Vancouver: UBC Press, 1992.
5. T. Christopher and E. L. Carstensen, Finite amplitude distortion and its relationship to linear derating formulae for diagnostic ultrasound devices. *Ultrasound Med. Biol.,* **22**: 1103–1116, 1996.
6. R. C. Preston, A. Shaw, and B. Zeqiri, Prediction of in situ exposure to ultrasound: an acoustical attenuation method; also Prediction of in situ exposure to ultrasound: a proposed standard experimental method. *Ultrasound Med. Biol.,* **17**: 317–339, 1991.
7. D. R. Bacon and A. Shaw, Experimental validation of predicted temperature rises in tissue-mimicking materials, *Phys. Med. Biol.,* **38**: 1647–1659, 1993.
8. M. E. Schafer and A. Broadwin, Acoustical characterization of ultrasonic surgical devices, *1994 Ultrason. Symp.,* New York: IEEE, 1994, p. 1903–1906.
9. P. A. Lewin et al., Characterization of optoacoustic surgical devices, *IEEE Trans. Ultrason. Ferroelectr. Freq. Control,* **43**: 519–526, 1996.
10. P. Lum et al., High-frequency membrane hydrophone. *IEEE Trans. Ultrason. Ferroelectr. Freq. Control,* **43**: 536–544, 1996.
11. B. Fay et al., Frequency response of PVDF needle-type hydrophones. *Ultrasound Med. Biol.,* **20**: 361–366, 1994.
12. B. Zeqiri and A. D. Bond, The influence of waveform distortion on hydrophone spatial-averaging corrections—theory and measurement. *J. Acoust. Soc. Am.,* **92**: 1809–1821, 1992.
13. G. R. Harris, Are current hydrophone low frequency response standards acceptable for measuring mechanical/cavitation indices? *Ultrasonics,* **34**: 649–654, 1996.
14. C. M. W. Daft et al., In-vivo fetal ultrasound exposimetry. *IEEE Trans. Ultrason. Ferroelectr. Freq. Control,* **37**: 501–505, 1990.
15. D. Royer and O. Casula, Quantitative imaging of transient acoustic fields by optical heterodyne interferometry. *Proc. 1994 Ultrason. Symp.,* p. 1153–1162, New York: IEEE, 1994.
16. J. Staudenraus and W. Eisenmenger, Fiber-optic probe hydrophone for ultrasonic and shock-wave measurements in water. *Ultrasonics,* **31**: 267–273, 1993.
17. B. Schneider and K. K. Shung, Quantitative analysis of pulsed ultrasonic beam patterns using a schlieren system. *IEEE Trans. Ultrason. Ferroelectr. Freq. Control,* **43**: 1181–1186, 1996.
18. G. R. Harris, M. R. Myers, and P. M. Gammell, The response of transiently-excited thick transducers at low frequencies. *J. Acoust. Soc. Am.,* **100**: 3115–3120, 1996.

GERALD R. HARRIS
Food and Drug Administration
PETER A. LEWIN
Drexel University

ULTRASONIC FILTERS. See ACOUSTIC MICROWAVE DEVICES.

ULTRASONIC FLOWMETERS. See FLOW TECHNIQUES, INDUSTRIAL.

ULTRASONIC IMAGING. See PIEZOELECTRIC DEVICES.

ULTRASONIC MICROMECHANICAL DEVICES. See ULTRASONIC AND ACOUSTIC MICROMECHANICAL DEVICES.